

# Plant-based production of highly potent anti-HIV antibodies with engineered posttranslational modifications

Advaita Acarya Singh<sup>1,3</sup>, Ofentse Pooe<sup>2</sup>, Lulusizwe Kwezi<sup>1</sup>, Therese Lotter-Stark<sup>4</sup>, Stoyan H. Stoychev<sup>1</sup>, Kabamba Alexandra<sup>1</sup>, Isak Gerber<sup>1</sup>, Jinal N. Bhiman<sup>8</sup>, Juan Vorster<sup>3</sup>, Michael Pauly<sup>5</sup>, Larry Zeitlin<sup>5</sup>, Kevin Whaley<sup>5</sup>, Lukas Mach<sup>7</sup>, Herta Steinkellner<sup>7</sup>, Lynn Morris<sup>6</sup>, Tsepo Lebiletsa Tsekoa<sup>1</sup> and Rachel Chikwamba<sup>1</sup>

## Supplementary Information

**Supplementary Figure S1.** Deconvoluted mass spectra of the HEK293-produced CAP256-VRC26.08 reduced light chain species.

**Supplementary Figure S2.** Deconvoluted mass spectra of the HEK293-produced CAP256-VRC26.08 reduced heavy chain species

**Supplementary Figure S3.** Deconvoluted mass spectra of the *N. benthamiana* ( $\Delta$ XTFT)-produced CAP256-VRC26.08 reduced light chain species.

**Supplementary Figure S4.** Deconvoluted mass spectra of the *N. benthamiana* ( $\Delta$ XTFT)-produced CAP256-VRC26.08 reduced heavy chain species.

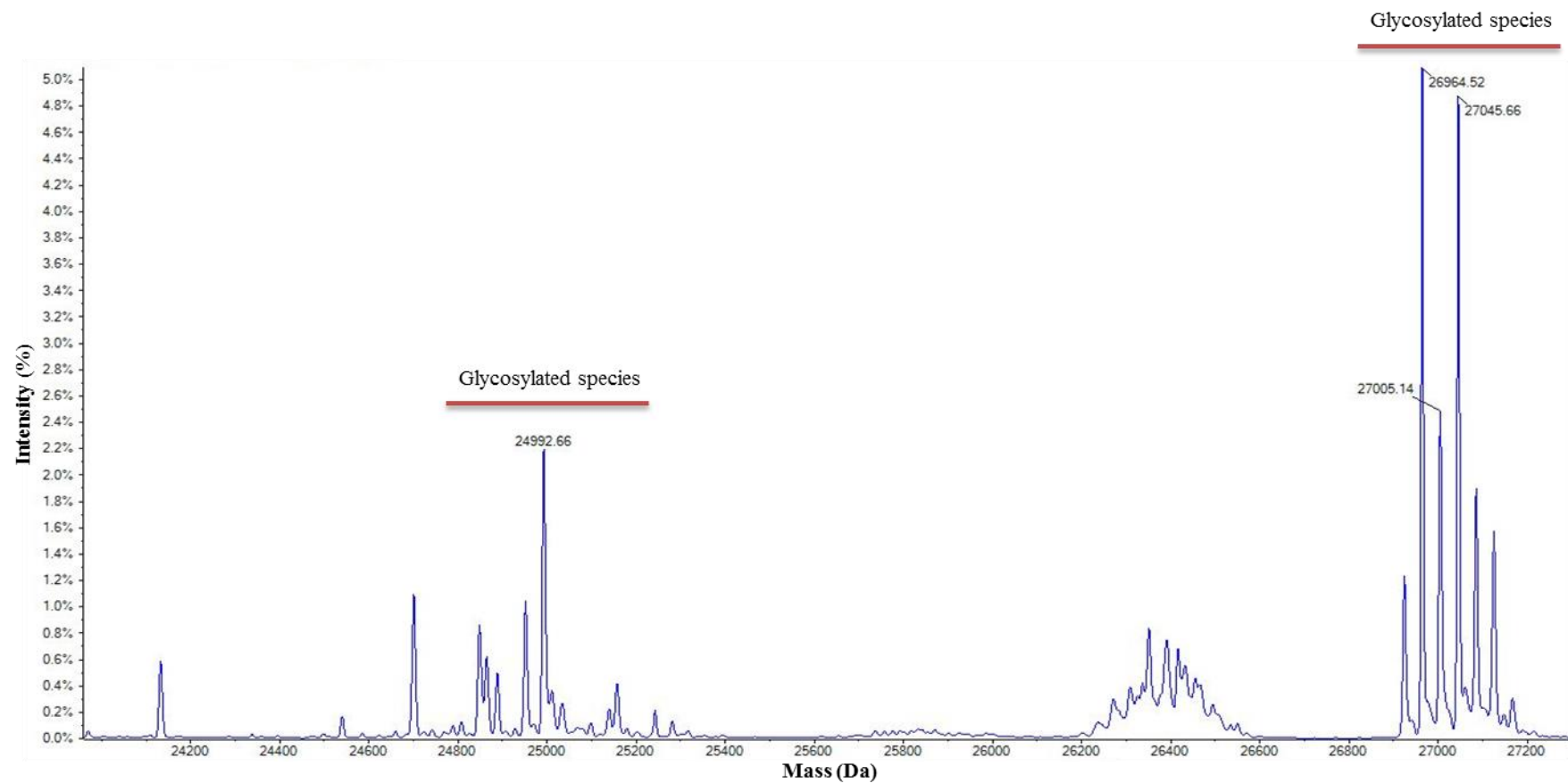
**Supplementary Figure S5.** Deconvoluted mass spectra of the HEK293-produced CAP256-VRC26.09 reduced light chain species.

**Supplementary Figure S6.** Deconvoluted mass spectra of the HEK293-produced CAP256-VRC26.09 reduced heavy chain species.

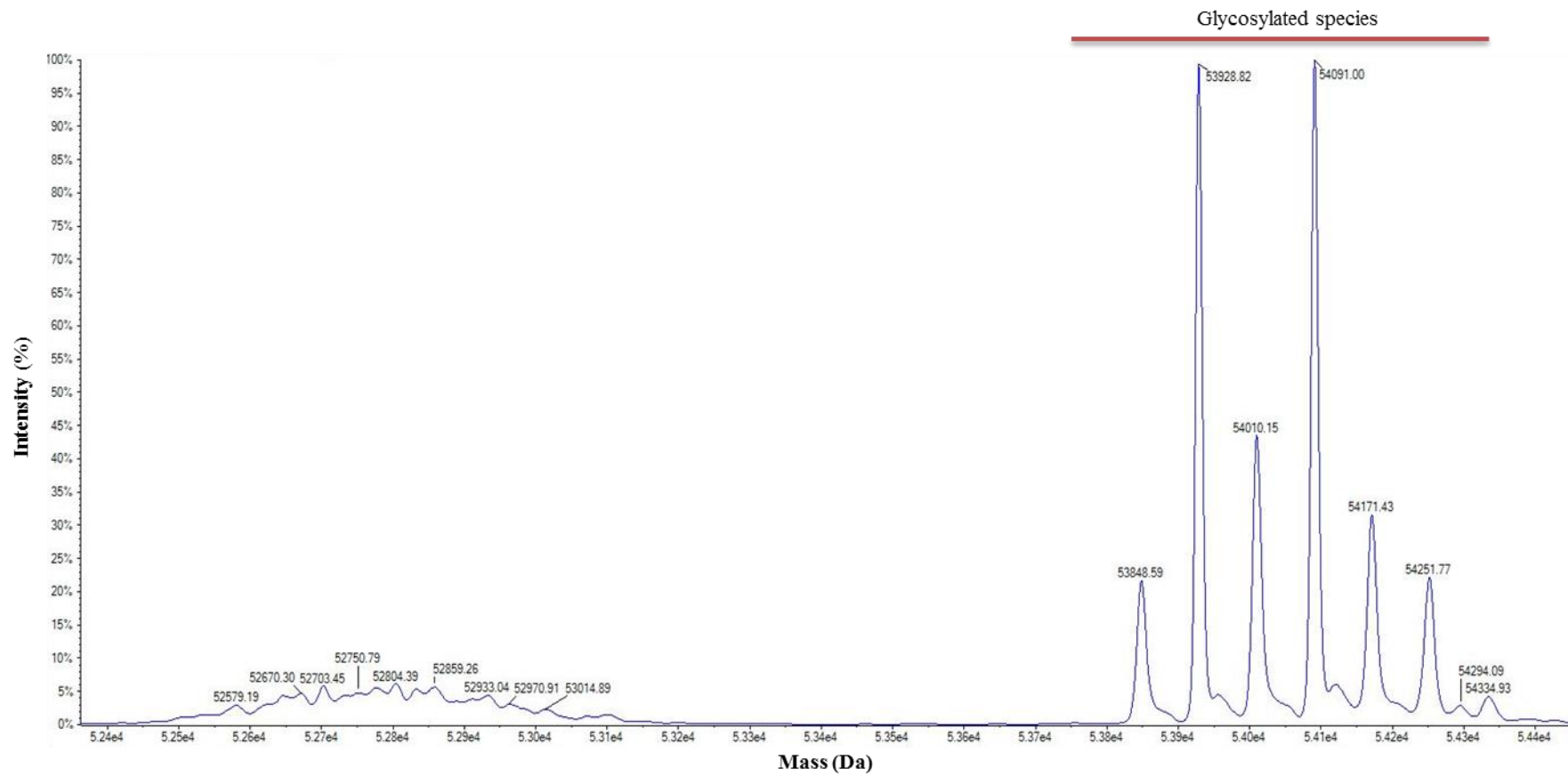
**Supplementary Figure S7.** Deconvoluted mass spectra of the *N. benthamiana* ( $\Delta$ XTFT)-produced CAP256-VRC26.09 reduced light chain species.

**Supplementary Figure S8.** Deconvoluted mass spectra of the *N. benthamiana* ( $\Delta$ XTFT)-produced CAP256-VRC26.09 reduced heavy chain species.

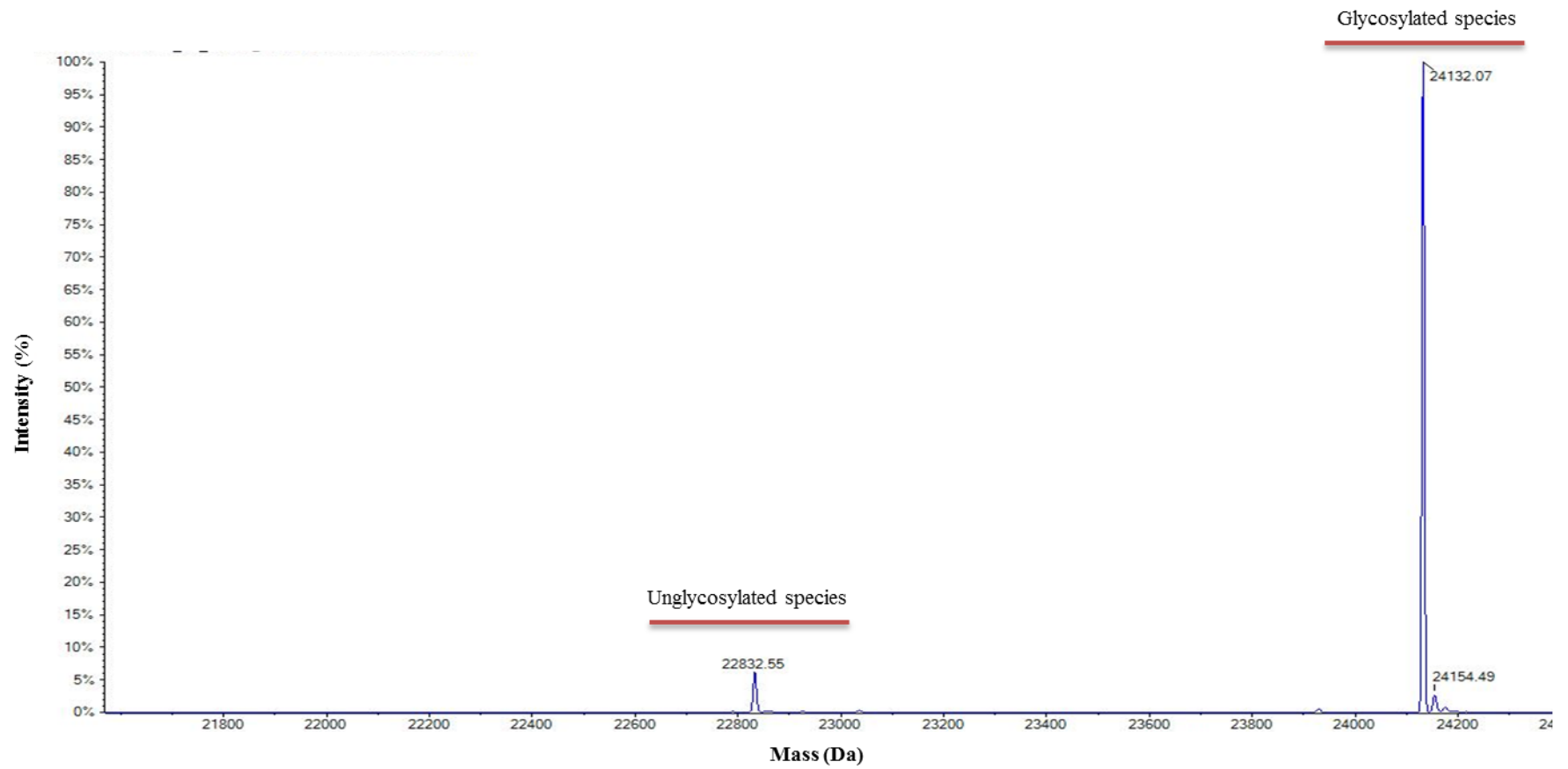
**Supplementary Figure S9.** Representative inhibition curves for the most sensitive virus of the subtypes C, B and A.



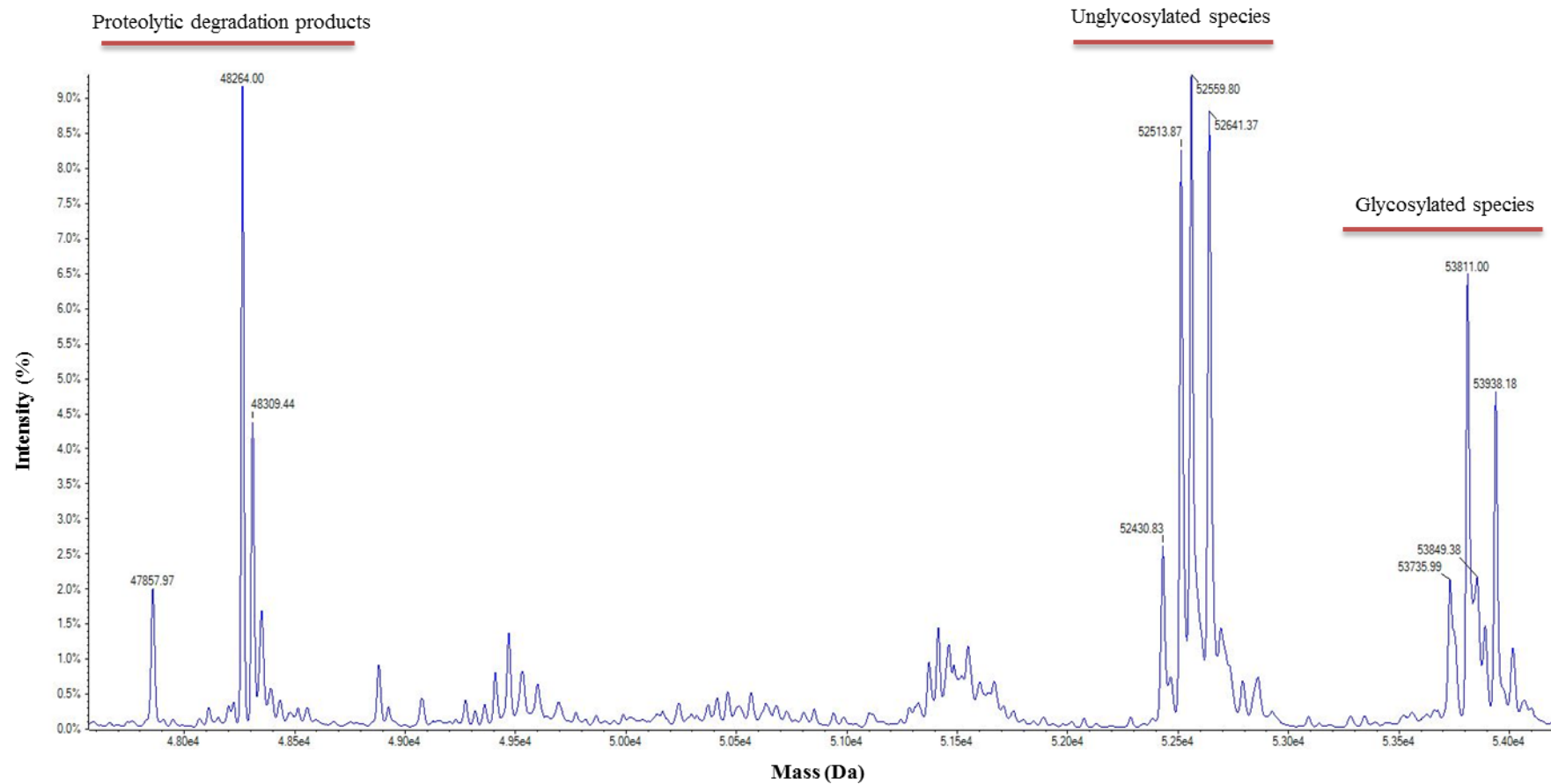
**Supplementary Figure S1.** Deconvoluted mass spectra of the HEK293-produced CAP256-VRC26.08 reduced light chain species.



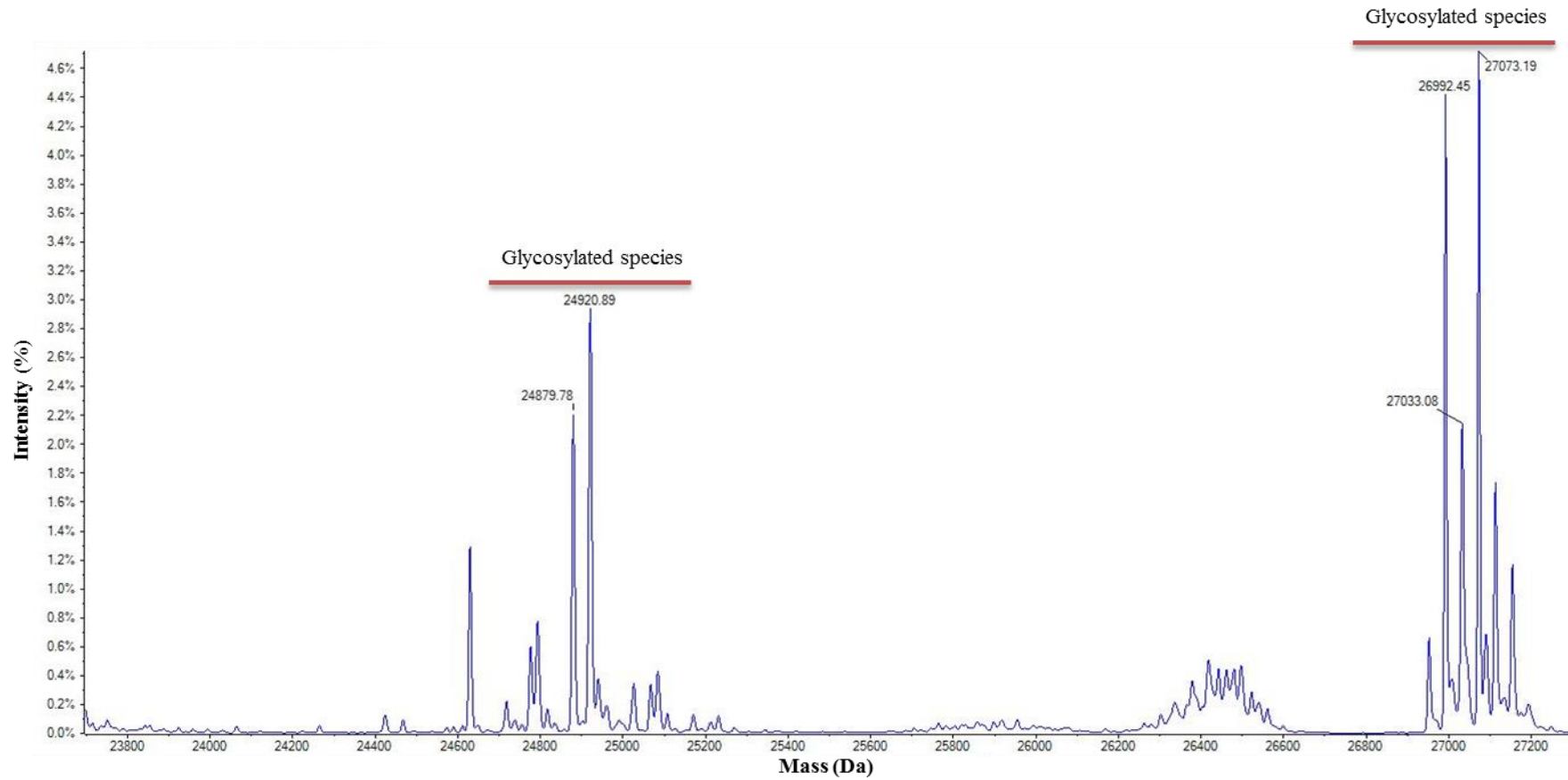
**Supplementary Figure S2.** Deconvoluted mass spectra of the HEK293-produced CAP256-VRC26.08 reduced heavy chain species.



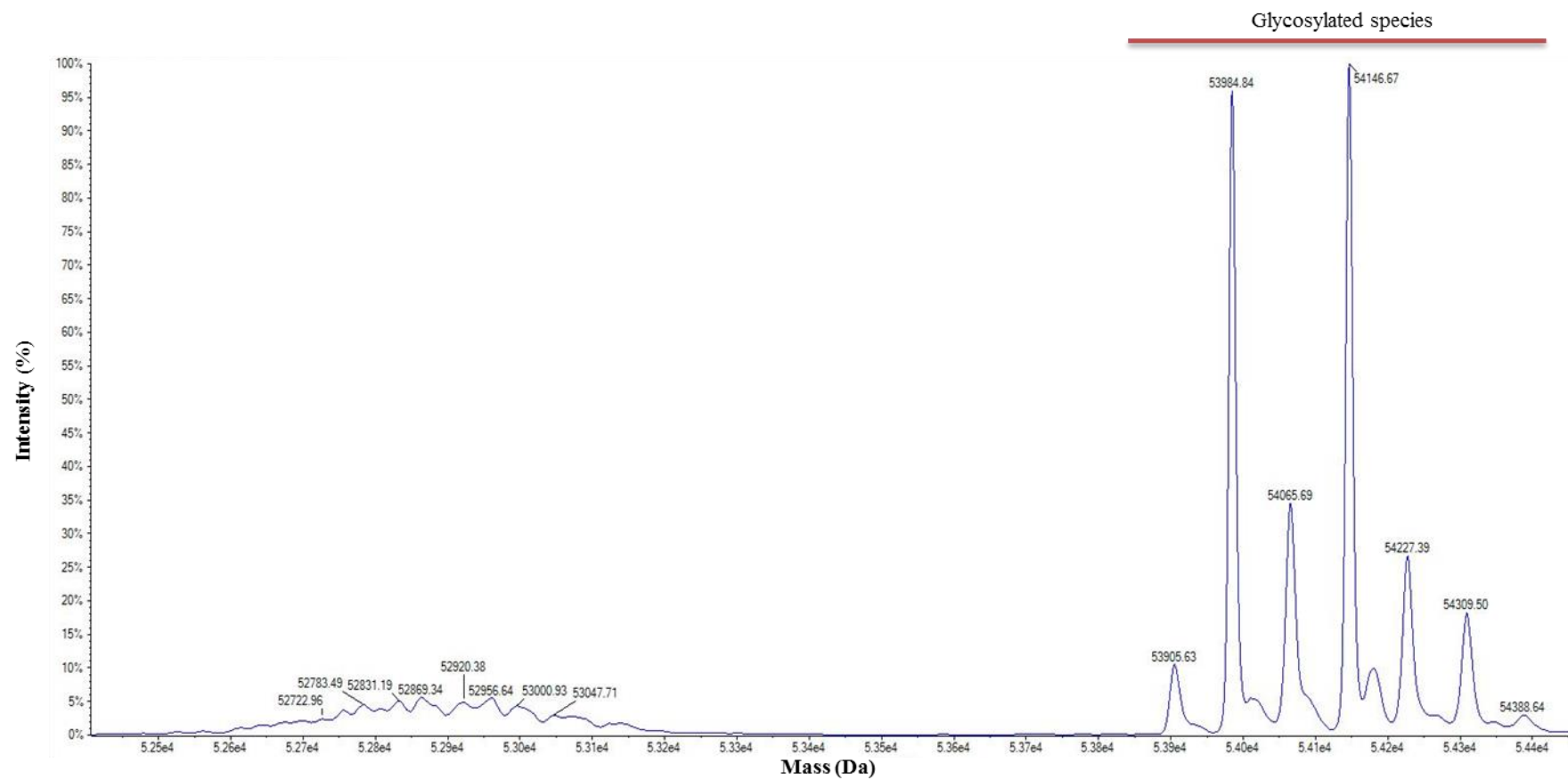
**Supplementary Figure S3.** Deconvoluted mass spectra of the *N. benthamiana* ( $\Delta$ XTFT)-produced CAP256-VRC26.08 reduced light chain species.



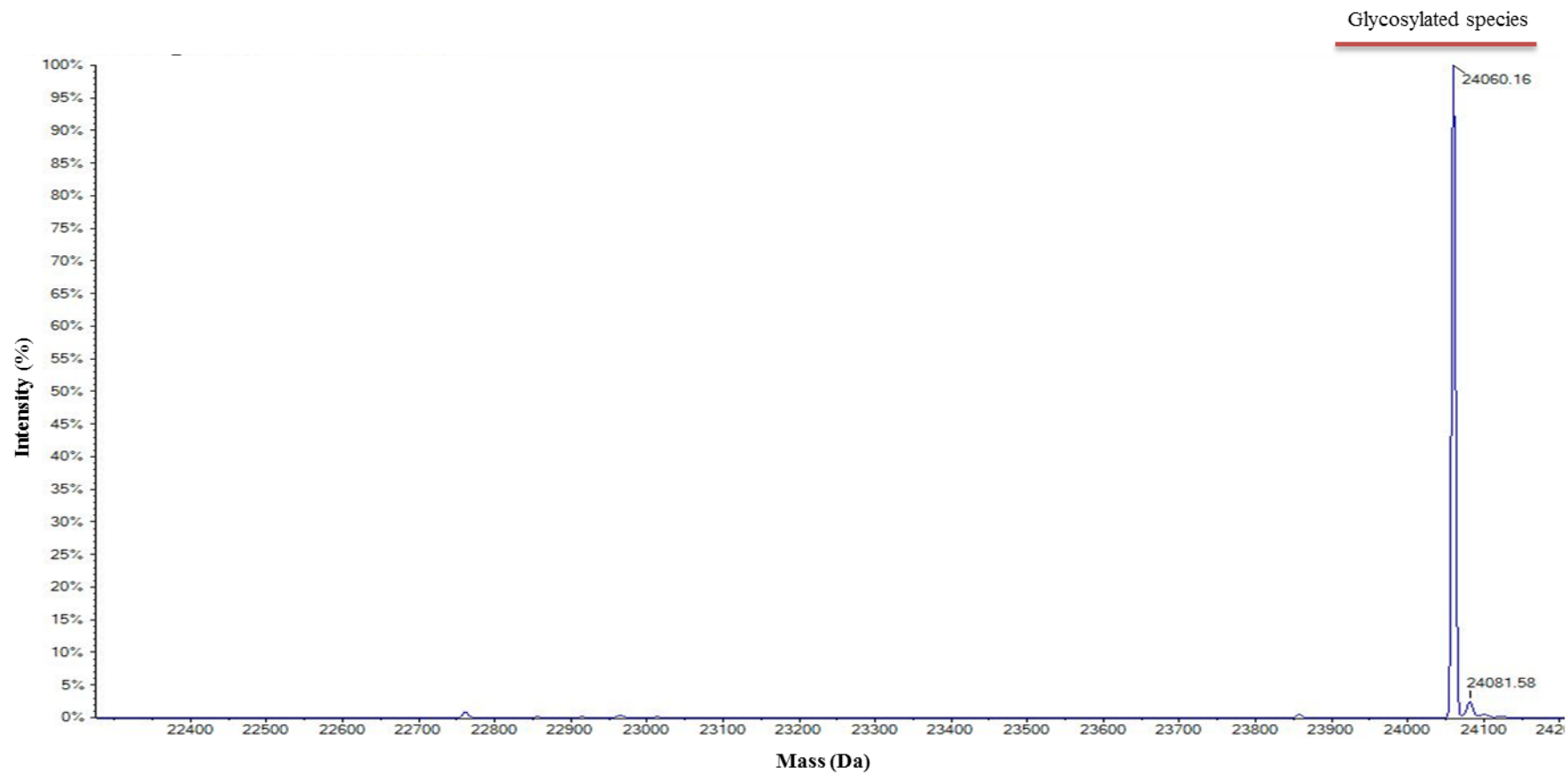
**Supplementary Figure S4.** Deconvoluted mass spectra of the *N. benthamiana* ( $\Delta$ XTFT)-produced CAP256-VRC26.08 reduced heavy chain species.



**Supplementary Figure S5.** Deconvoluted mass spectra of the HEK293-produced CAP256-VRC26.09 reduced light chain species.

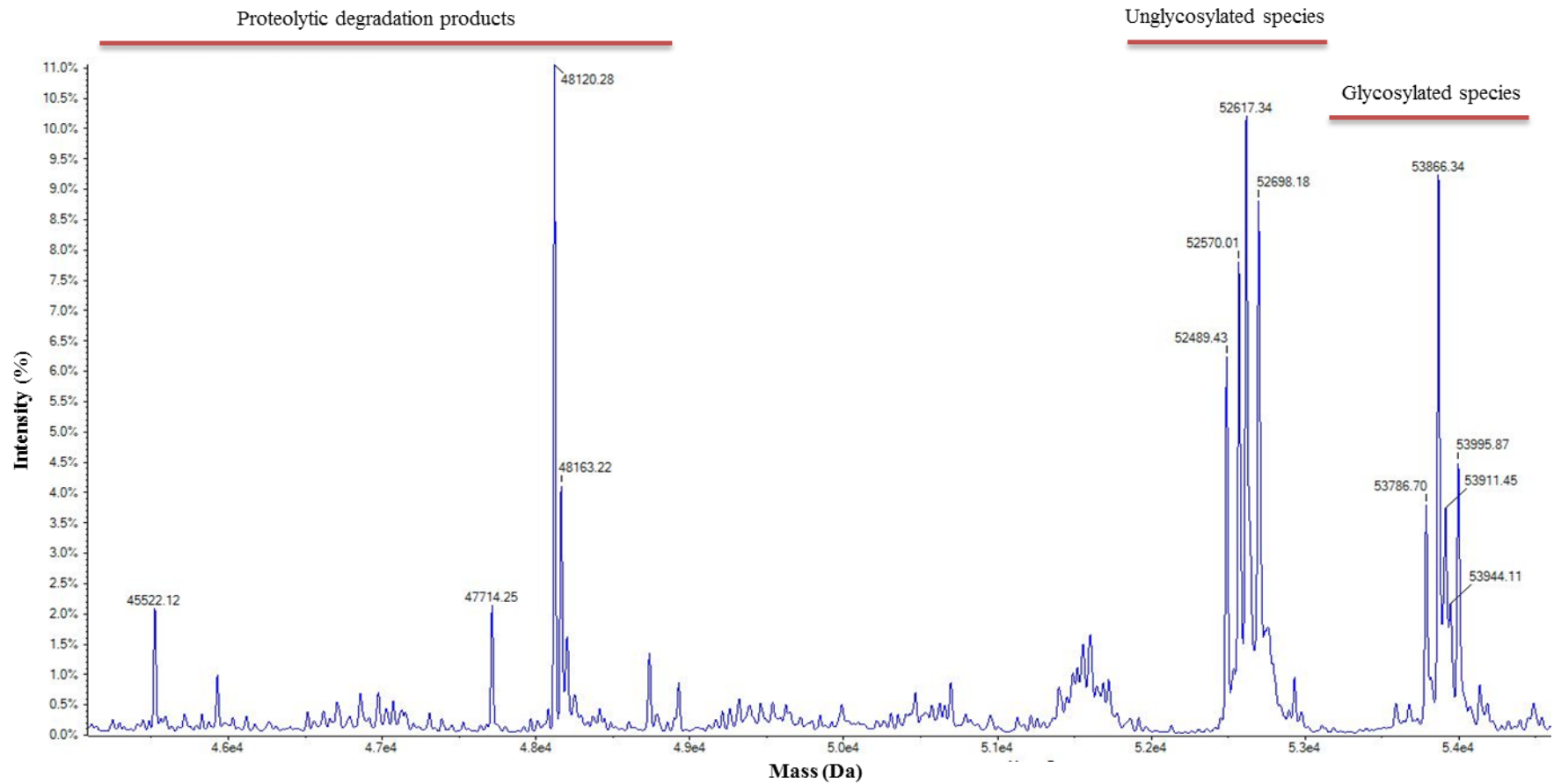


**Supplementary Figure S6.** Deconvoluted mass spectra of the HEK293-produced CAP256-VRC26.09 reduced heavy chain species.

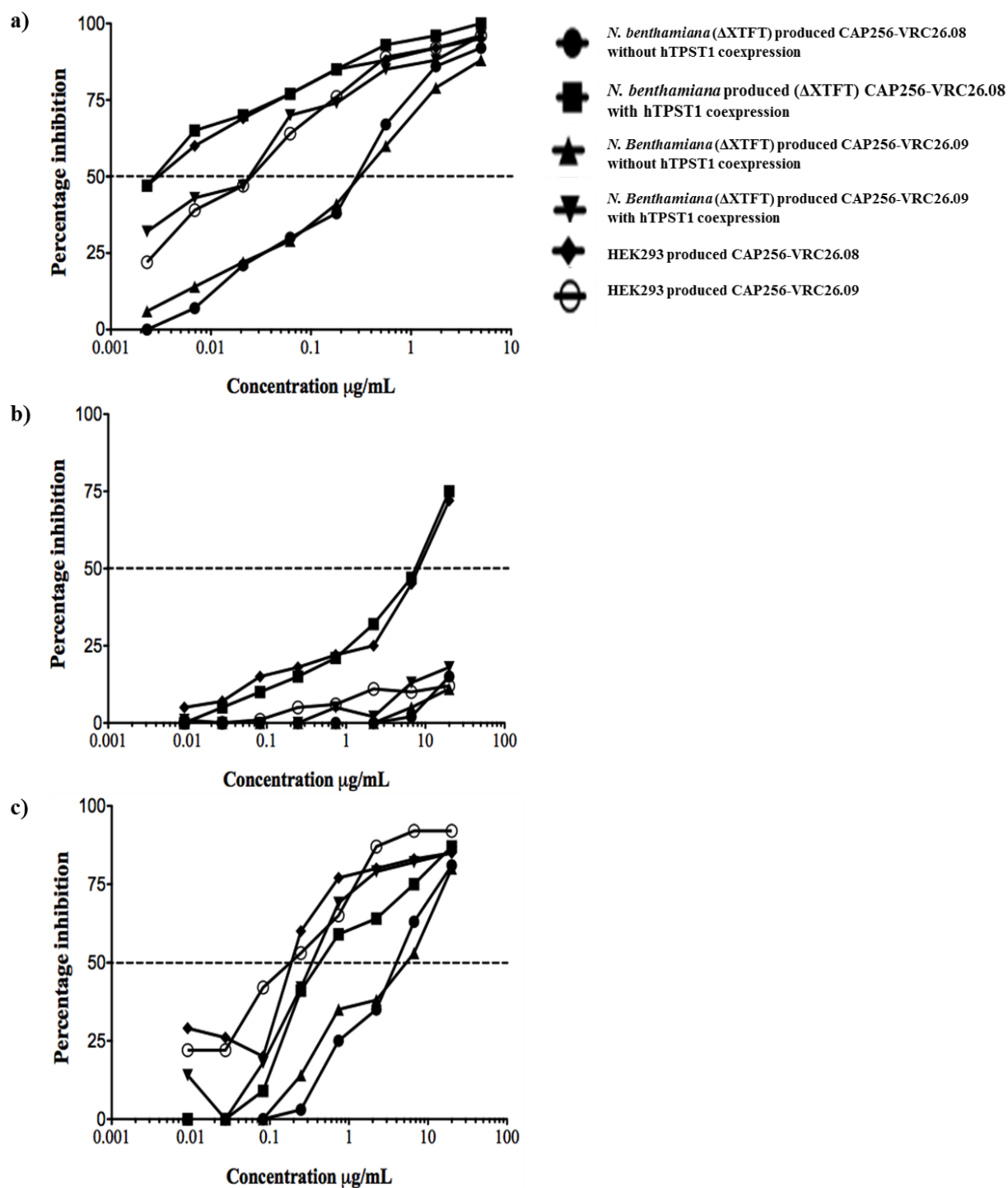


**Supplementary Figure S7.** Deconvoluted mass spectra of the *N. benthamiana* ( $\Delta$ XTFT)-produced CAP256-VRC26.09 reduced light chain species.





**Supplementary Figure S8.** Deconvoluted mass spectra of the *N. benthamiana* ( $\Delta$ XTFT)-produced CAP256-VRC26.09 reduced heavy chain species.



**Supplementary Figure S9.** Representative inhibition curves for the most sensitive virus for the subtypes C, B and A. Inhibition curves used to calculate the  $\text{IC}_{50}$  values of (a) the subtype C virus Du422.1, (b) the subtype B PVO.4, and (c) the subtype A Q168.a2 following the TZM-bl cells neutralization assay. Dashed lines are placed at 50% inhibition of HIV-1 infection.